^{31}P NMR AND TWO-DIMENSIONAL NMR SPECTRA OF NUCLEIC ACIDS AND 2D NOESY-CONSTRAINED MOLECULAR MECHANICS CALCULATIONS FOR STRUCTURAL SOLUTION OF DUPLEX OLIGONUCLEOTIDES[#]

DAVID G. GORENSTEIN*, STEPHEN A. SCHROEDER*, MITSUE MIYASAKI[‡], JOSEPHA M. FU*, VIKRAM ROONGTA*, PERLETTE ABUAF[‡], JAMES T. METZ*, and CLAUDE R. JONES*

Departments of Chemistry, Purdue University* and University of Illinois at Chicago[‡], W. Lafayette IN 47907 and Chicago IL 60680

INTRODUCTION

Nuclear magnetic resonance spectroscopy is now able to provide detailed 3-dimensional structures and dynamics of oligonucleotide duplexes and nucleic acid complexes (1,2). Unfortunately, of the six torsional angles that largely define the backbone structure, only the four involving the deoxyribose ring have been shown to be directly amenable to analysis by NMR techniques. In fact for modest-sized oligonucleotide duplexes, determination of these torsional angles through measurement of three-bond coupling constants is very difficult. Using the time development of cross peak intensities in 2D-NOESY NMR spectra, a number of workers (3-10) have been able to qualitatively or semi-quantitatively determine whether two protons are within 3-5 Å of each other (11). From these NOESY-derived distances and constrained molecular dynamics or distance geometry (12) calculations, models for these duplexes may be determined. While base pairing and stacking interactions can often be adequately demonstrated, detailed conformational information, especially with regard to the deoxyribose phosphate backbone, is often lacking.

We have proposed that ^{31}P NMR spectroscopy is capable of providing information on the most important remaining two torsional angles involving the phosphate ester bonds. Our studies (see refs 13-20) indicated that a phosphate diester monoanion in a gauche, gauche (g,g) conformation should have a ^{31}P chemical shift 1.5-2.5 ppm upfield from an ester in a non-g,g conformation. In this review ^{31}P NMR and two dimensional ^{1}H NMR methods, COSY and NOESY in particular, will be used to examine the three-dimensional structure of various oligonucleotide and an oligonucleotide drug complex.

^{31}P NMR OF OLIGONUCLEOTIDES

Recently we have used a ^{17}O/^{18}O-phosphorylation scheme to identify the ^{31}P resonances of oligonucleotides (10,20). Using the solid-phase phosphite triester method, we have synthesized deoxyoligonucleotides 1 - 4. We can readily introduce ^{17}O (or ^{18}O) labels into the phosphoryl groups

$(dAGCT)_2$	dCGCAGAATTC-GCG dGCG-CTTAAGACGC
1	2
dCGTGAATTCGCG dGCGCTTAAGTGC	dTGTGAGCGCTCACA dACACTCGCGAGTGT
3	4
	lac pseudo-operator

by replacing the I_2/H_2O in the oxidation step of the phosphite by $I_2/H_2{}^{17}O$ (40%)or $I_2/H_2{}^{18}O$ (20-22). Similarly, Stec et al. (23)have replaced one of the nucleoside phosphates by a nucleoside thiophosphate by using sulfur/2,6-lutidine in the oxidation step at the appropriate cycle. By synthesizing the

[#]Presented in part at the Waterloo NMR School, June 10-15, 1985, Waterloo, Ontario, Canada

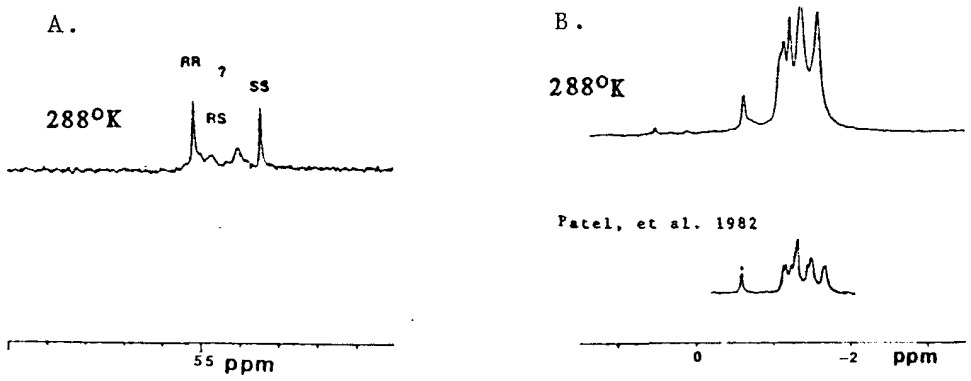

Figure 1. ^{31}P NMR spectra at indicated temperatures of thiophosphoryl labeled 13-mer 2 (A) $^{31}P(S)$ region, (B) $^{31}P(O)$ region.

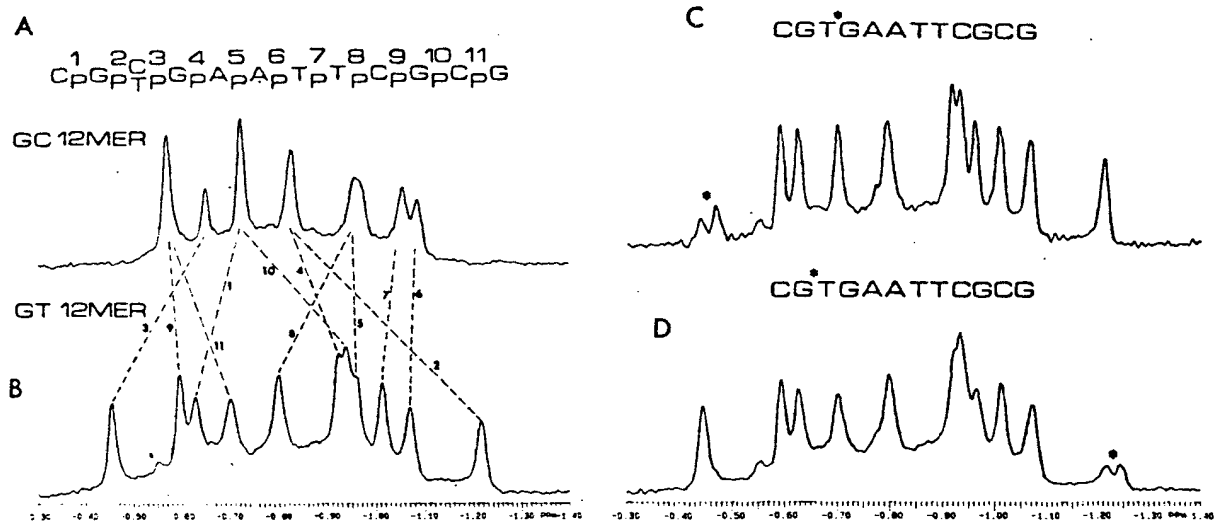

Figure 2. ^{31}P NMR spectra of (A) CG-12 mer duplex $d(CGCGAATTCGCG)_2$ and (B) GT-12-mer duplex 3. Examples of ^{17}O labeled duplex 3 are shown in (C) and (D)

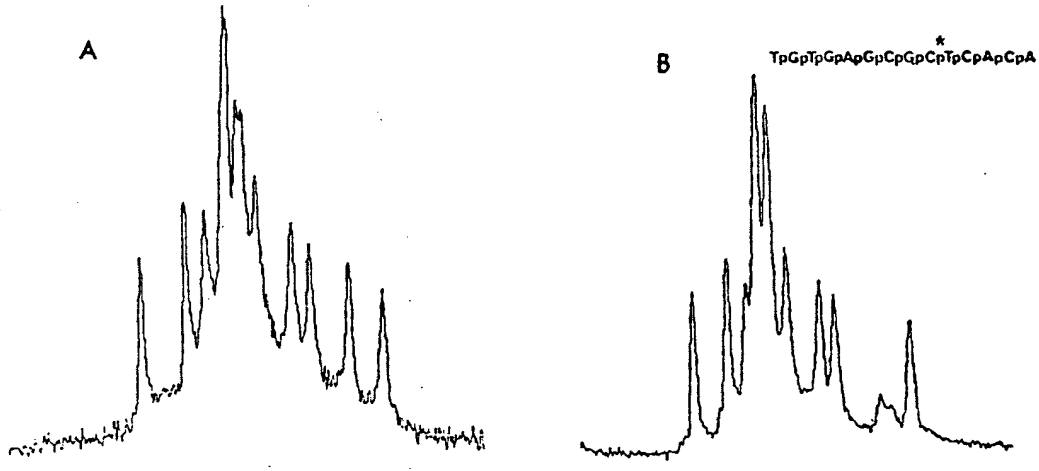

Figure 3. P-31 NMR spectra of 14-mer 4 (A) and O-17 labeled 14-mer at indicated position.

corresponding mono-^{17}O phosphoryl labeled oligonucleotide (each phosphate is separately substituted along the chain), we can identify the ^{31}P signal of that phosphate diester. The quadrupolar ^{17}O nucleus (generally ca. 40% enriched) broadens the ^{31}P signal of the directly attached phosphorus to such an extent that only the high-resolution signal of the remaining 60% non-quadrupolar broadened phosphate at the ^{17}O-labeled site is observed (20-22). In this way each synthesized oligonucleotide with a different monosubstituted ^{17}O-phosphoryl group allows identification of all phosphate ^{31}P signals.

Patel and coworkers (24) have shown that base insert and mismatch in duplexes 2 and 3 provide very interesting ^{31}P spectral shifts. Whereas the ^{31}P spectral dispersion is < .6 ppm in normal B-DNA double helices 1 and 4, new signals are shifted upfield and downfield from the "normal" double helical phosphate ^{31}P signals with a total spread > 1 ppm in duplexes 2 and 3. By ^{17}O and S labeling we have been able to assign these perturbed ^{31}P signals to phosphates in non-Watson-Crick regions of the duplexes (Figures 1 and 2).

As shown in Figure 1A, sulfur substitution into the dCpG phosphodiester between residues 10 and 11 produces several new ^{31}P signals ca. 55 ppm downfield from the unmodified phosphodiester signals resonating at ca. -1 ppm (Figure 1B). Sulfur substitution introduces a new chiral center, and since the 13S-mer is self-complementary, the duplex results in four diastereomers: RR, RS, SR and SS. The P-S region of the ^{31}P NMR spectrum of the 13S-mer therefore shows four signals (23). As in the ^{31}P NMR study of the unlabeled 13-mer by Patel et al., (ref. 24; spectrum shown at the bottom of Figure 1B) the ^{31}P NMR spectrum of the 13S-mer shows a resolved signal which is ca. 0.5 ppm downfield from the main cluster. This resolved signal integrates for one phosphodiester at room temperature relative to the integration of ten phosphodiesters for the whole main cluster. The four signals in the P-S region together integrate for ca. 90% of a single phosphodiester. The resolved downfield peak at 0.5 ppm downfield is still observed in the ^{31}P NMR spectra of the 13S-mer. One might argue that a thiophosphate can perturb the conformation of the oligodeoxynucleotide and thus make it difficult to assign the ^{31}P NMR chemical shifts of the unsubstituted phosphates. However, the magnitude of the chemical shift differences in the neighboring phosphodiester region in a thiophosphoryl labeled phosphodiester are known to be rather small (ref. 25; less than 0.2 ppm, also see below). In Patel's 13-mer, however, the resolved phosphodiester chemical shift is ca. 0.45 ppm downfield from the main cluster. Thus the phosphothioate substitution in the 13-mer has established that this downfield shifted ^{31}P signal at 0.5 ppm does not belong to the dCpG phosphate opposite the extra dA residue at position 10, as originally suggested by Patel et al. (24).

Assignment of all of the phosphates in the GT base mismatch 12-mer 3 has followed the ^{17}O-labeling methodology. Examples of some of the ^{17}O-phosphoryl labeled 12 mer 3 is shown in Figure 2, as well as a comparison of the ^{31}P resonance assignments for the Dickerson base-paired GC-12-mer d(CGCGAATTCGCG) and the GT mismatch 12-mer 3 (the GC-12 mer assignments are from ref. 22). In general the ^{31}P chemical shifts of those phosphates in 12-mer 3 furthest from the mismatch sites at position 3 from both 5′ ends of the duplex are quite similar to those of the GC-12-mer. The two signals shifted the most upfield GpT phosphate at (position 2) and downfield (TpG phosphate at position 3) occur at the site of mismatch.

Assignment of most of the ^{1}H (described in a separate section below) and all 13 ^{31}P signals of the tetradecamer 4 has also followed the ^{17}O-labeling, 2-D NMR methodology (10).

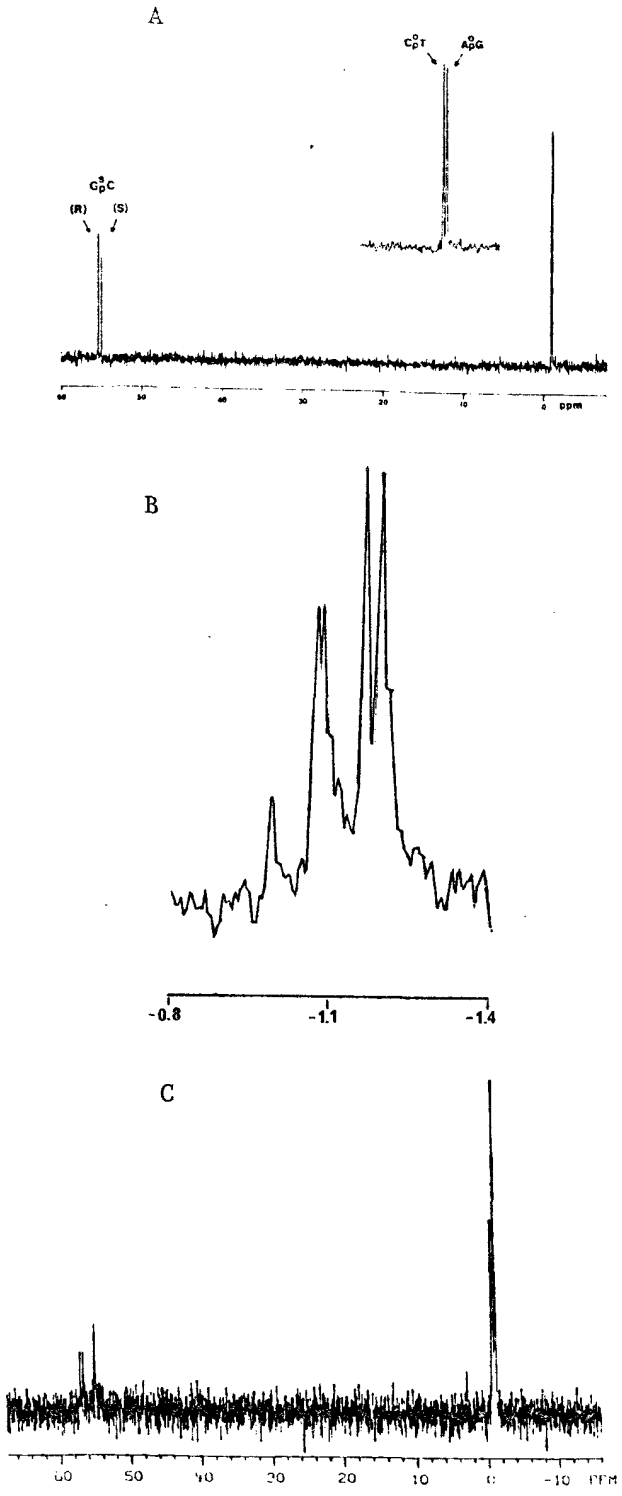

Figure 4. (A) ^{31}P NMR spectrum of d(AG(S)CT) at 81.0 MHz, 24 C; (B) expansion of upfield region at 162 MHz; (C) ^{31}P NMR spectrum of actinomycin D d(AG(S)CT duplex at 162 MHz, 50^{o} C.

Thus as shown in Figure 3, the ^{31}P NMR spectra of various regio-specifically labeled phosphates in the duplex 4 allow clear assignment of the ^{31}P signals.

By using ^{17}O and thiophosphoryl-labeling of the oligonucleotides we can also determine the site and detailed structure of drug binding to oligonucleotides. Thus as confirmed by ^{31}P NMR studies of Petersheim et al. (21) and our laboratory (20b) actinomycin D has specificity for G-C base pairs and as Patel (24) had earlier shown two ^{31}P signals are shifted 1.4-2.6 ppm downfield from the other signals in the actinomycin D complexes of d(CGCG) and d(ATGCAT). Our earlier study used ^{17}O-labeling and more recently (26) we have been able to use thiophosphoryl-labeling to confirm the ^{31}P signal assignments in the actinomycin D d(AGCT) duplex complex. The ^{31}P NMR spectrum of d(AG(S)CT) is shown in Figure 4a (G(S)C denotes thiophosphoryl-labeling in the GpC phosphate). Because of the thiophosphoryl-labeling, the Gp(S)C phosphate ^{31}P signal is shifted to ca. 55 ppm. At 24^{o} C the tetramer exists largely in the single strand state and thus unlike the thiophosphoryl-labeled 13-mer discussed above, we only observe ^{31}P signals for the S and R configuration thiophosphates at 54.98 and 55.40 ppm, respectively. The upfield region of the ^{31}P NMR spectrum of d(AG(S)C(O-17)T) is shown in Figure 4(B). This double-labeled tetramer (S labeling on the GpC phosphate and O-17 labeling on the CpT phosphate), has been used to confirm the assignments of the ^{31}P signals shown in Figure 4(A). Thus the the small downfield signal at -0.99 ppm may be assigned to the residual Gp(O-16)C phosphodiester: it integrates for about 10% of one phosphodiester since the thiophosphoryl oxidation step is about 90% complete. The "doublet" signal at -1.09 ppm is lower in intensity than the most upfield "doublet signal" signal at -1.19 ppm due to the incorporation of O-17 into the CpT phosphate. Thus the CpT phosphate can unambiguously be assigned

to the signals at -1.09 ppm and the ApG phosphate to the signals at -1.19 ppm. For comparison, the ^{31}P chemical shifts of the signals for the unlabeled tetramer are -1.22, -1.06, and -0.96 ppm for the ApG, CpT, and GpC phosphates, respectively (20). This again demonstrates that sulfur substitution produces less than 0.1 ppm perturbation in the ^{31}P chemical shifts of non-sulfur labeled phosphates. Interestingly, the ApG and CpT signals shown in Figure 4(B) appear as "doublets", presumably due to the slight difference in the magnetic environments of the phosphates in the R and S diastereomers created by sulfur substitution at a remarkably remote site.

As described above, perturbation of the ^{31}P signal of the GpC phosphates has been used to confirm the intercalative binding of actinomycin D to duplex DNA (20b, 21). Similar perturbations in the ^{31}P NMR spectrum of d(AG(S)CT) upon binding actinomycin D have also been observed (26). Most interestingly, as shown in Figure 4(C), it appears that only one of the thiophosphate tetramer diasteromers binds the intercalating drug. It appears as though the ^{31}P signal of the R diasteromer at 55.4 ppm shifts downfield by 1.3 and 1.8 ppm in the duplex drug complex. In contrast the S thiophosphate diastereomer tetramer signal at 54.98 ppm shows only a small downfield shift upon addition of actinomycin D to the sample. In our earlier actinomycin D tetramer duplex ^{31}P NMR study the GpC phosphate signals shifted 1.4 and 2.6 ppm downfield from the free tetramer signal (note that in both the unlabeled and thiophosphate tetramer drug complexes, the GpC phosphate in one strand is in a different conformation than the GpC phosphate in the other strand, reflecting the asymmetry introduced into the duplex complex by the asymmetric drug.)

^{31}P CHEMICAL SHIFTS AND CALLADINE'S RULES

A number of studies have been carried out to gain insight into the various factors responsible for ^{31}P chemical shift variations in oligonucleotides (14,16,17,22). As discussed above, one of the major contributing factors that determine ^{31}P chemical shifts is the main chain torsional angles of the individual phosphodiester groups along the oligonucleotide double helix. Phosphates located towards the middle of a B-DNA double helix assume the lower energy gauche,gauche conformation, while phosphodiester linkages located towards the two ends of the double helix tend to adopt a mixture of g,g and g,t conformations, where increased flexibility of the helix is more likely to occur. Because the g,g conformation is responsible for a more upfield ^{31}P chemical shift, while a g,t conformation is associated with a lower field chemical shift, internal phosphates in oligonucleotides would be expected to be upfield of those nearer the ends. Although several exceptions have been observed, this positional relationship appears to be generally valid in oligonucleotides for which ^{31}P chemical shift assignments have been determined (10,22). Thus position of the phosphorus within the oligonucleotide is one important factor responsible for ^{31}P chemical shifts.

Ott and Eckstein (22) have recently suggested that while nucleotide base sequence does not seem to be a major contributing factor affecting ^{31}P chemical shifts (see also ref. 14), the occurrence of a pyrimidine-purine base sequence does. It appears that 5′-PyPu-3′ dinucleotide sequences within the oligonucleotide have a more downfield than expected ^{31}P chemical shift if based solely on the phosphate positional relationship. An explanation for these anomolous chemical shifts is based on structural considerations of the double helix as proposed by Calladine (27). In essence, local helical distortions (28) arise along the DNA chain due to purine-purine steric clash on opposite

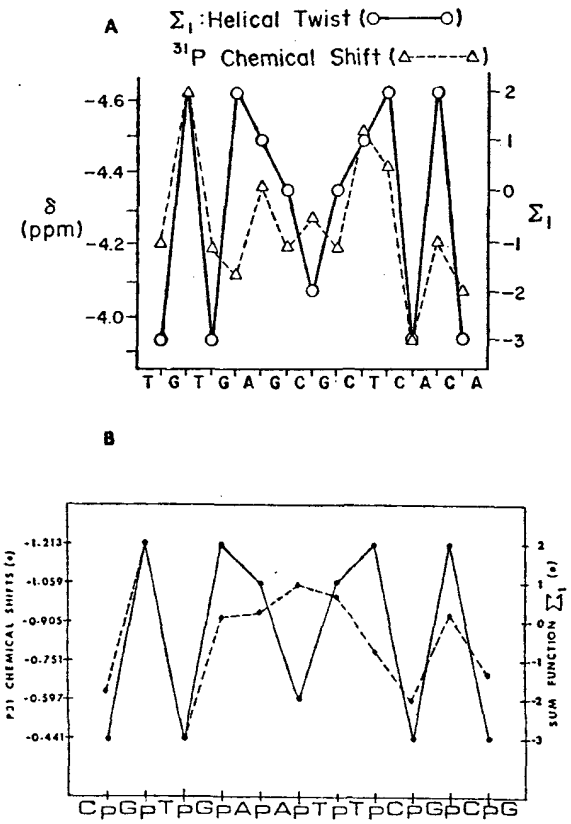

Figure 5. Correlation of Dickerson/Calladine rule sum function for local helical twist and ^{31}P chemical shifts for (A) 14-mer 4 and (B) GT-mismatch 12-mer 3.

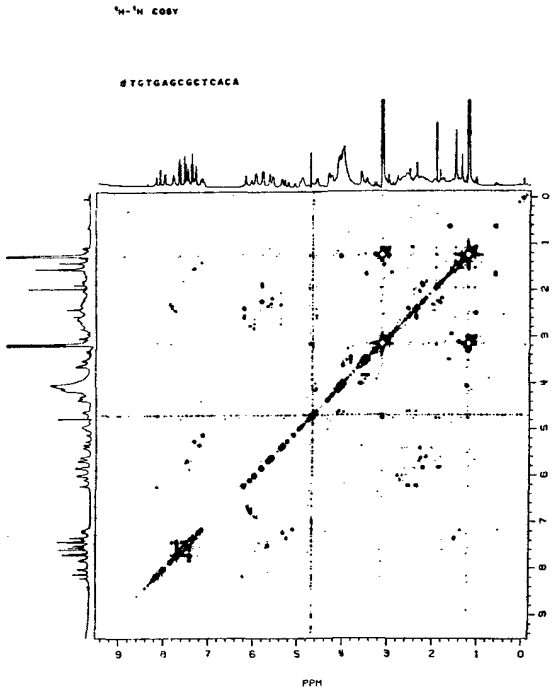

Figure 6. Absolute value ^{1}H-^{1}H COSY NMR spectrum of duplex 14-mer, d(TGTGAGCGCTCACA)$_2$, at 470 MHz.

strands of the double helix. As a result, 5′-PyPu-3′ sequences within the oligonucleotide represent positions where the largest helical distortions occur. This appears to be another important factor that influences ^{31}P chemical shifts.

Since the discovery of sequence dependent structural distortions that occur along the oligonucleotide backbone, is it likely that any correlation or relationship exists between ^{31}P chemical shifts and these local helical distortions? Eckstein and Ott have proposed, based on the ^{31}P assignments of two dodecamers, that a correlation exists between roll angle and ^{31}P chemical shifts (22). No significant correlation is apparent for the other three Dickerson/Calladine sum functions. However, from the ^{31}P assignments of our 12-mer 3 and 14-mer 4, there does appear to be a modest correlation with the helical twist sum function, as shown in Figure 5.

Surprisingly, the GT-mismatch 12-mer duplex 3 also shows a good correlation between the helix twist sum function and the ^{31}P chemical shift. In contrast the normal GC-12 mer does not show a very good correlation with this sum function (22). Most significantly, the two positions least expected to show these sorts of correlations (the two phosphates adjacent to the mismatch site), show very good correlations with the sum functions. This further substantiates the point that ^{31}P chemical shifts in these duplexes reflects in some way the local geometry of the duplex, independent of the exact chemical structure of the base.

^{1}H NMR OF OLIGONUCLEOTIDES

Assignment of the proton signals of the oligonucleotide duplexes was accomplished through analysis of the two-dimensional COSY and NOESY NMR spectra following a sequential assignment methodology (3,4,7,8,10). In the COSY spectrum (Figure 6 of the 14 bp duplex 4, scalar couplings between protons are manifested as off-diagonal cross peaks. Each of the four cytosines, in one of the symmetrical halves of the spectrum, gives rise to a cross peak representing the H5-H6 coupling (region A). Similarly, the long range H5-CH_3 couplings in the three thymines give rise to the cross peaks in region B. No cross peaks from the purine bases are present since adenine and guanine do not possess groups of coupled non-exchangeable protons. The various couplings among the deoxyribose protons, i.e. H1′-H2′, 2", H2′2"-H3′, H3′-H4′, H4′-H5′, 5" may be traced through their COSY connectivities.

While the COSY spectrum can be used to assign the protons on a particular base or sugar, it does not provide any information on the relative position of the base or sugar in the 14-mer sequence. This information can be obtained, however, through analysis of the cross-relaxation networks delineated in the NOESY spectrum (Figure 7). Because the NOESY experiment (11) utilizes through-space connectivities rather than through-bond connectivities, correlations between base and sugar protons on neighboring residues can be be seen. This NOE information, taken together with the type of base assignments from the COSY spectrum, and compared to the known sequence of the 14-mer, permitted assignment of nearly all the protons in the lac pseudo-operator segment.

In B-DNA, each pyrimidine H6 or purine H8 base proton is spatially situated so as to give rise to an NOE correlation with the H1′ sugar proton of the same nucleotide as well as with the H1′ sugar proton of the adjacent nucleotide on the 5′ side (region A).

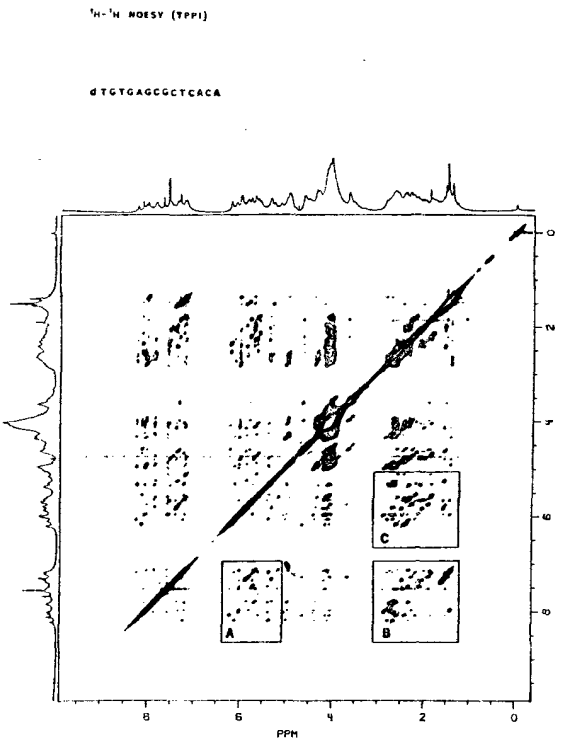

Figure 7. Pure absorption phase ^{1}H-^{1}H NOESY NMR spectrum of duplex 14-mer, at 470 MHz.

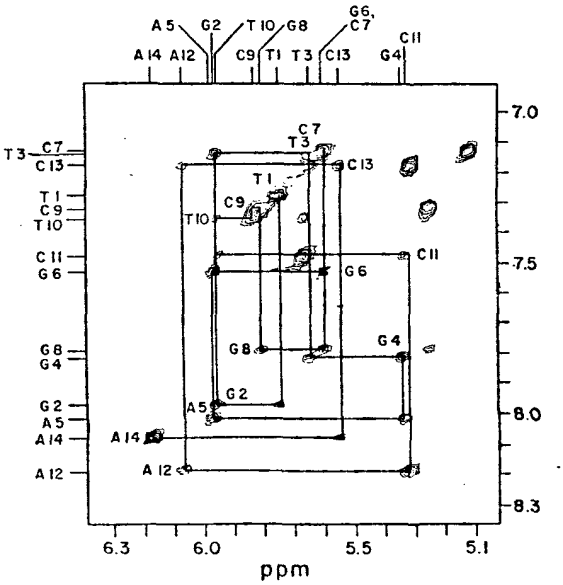

Figure 8. Expansion of region A of the NOESY spectrum shown in Figure 7. The sequential assignment of the base and deoxyribose H1′ protons is diagrammed.

The base at the 5′ end of the chain can be identified by its lack of an NOE cross peak to a 5′ neighboring sugar H1′ proton, and the sugar H1′ proton at the 3′ end can be identified by its lack of an NOE cross peak to a 3′ neighboring base proton. Using these as starting points, it was possible to step through the entire helix via the sugar-base-sugar connectivities, as diagrammed in Figure 8. The thus assigned sugar H1′ protons are, in turn, correlated to the H2′ and 2" protons of the same nucleotide, allowing these to be assigned(10). Once the assignments of the sugar H1′ and H2′, 2" and the base protons were known, the H3′ protons were identified through their NOE correlations to these protons. The H4′ protons were assigned through their connectivities with H1′.

^{31}P - ^{1}H HETERONUCLEAR SHIFT CORRELATION (COLOC) NMR SPECTRA

Some of the H5′ and H5" protons were assigned as a group, but complete assignment was not possible because of inadequate resolution in the NOESY and COSY spectra. However, additional assignments of the H5′ and H5" protons and verification of the H3′ assignments were achieved through analysis of the two-dimensional ^{31}P - ^{1}H heteronuclear shift correlation (HETCOR) NMR spectrum (or more recently the COLOC NMR spectrum, Figure 9). Three-bond scalar couplings between the ^{31}P nuclei in the phosphate backbone and the H3′, H5′, and H5" deoxyribose protons are manifested as cross peaks in this spectrum. Since we know the nucleoside to which the ^{31}P signal is associated by P=S or P=$^{17}O/^{18}O$ labeling, we are able to identify the ^{1}H signals coupled to this phosphorus atom (H3′, H5′, H5" via $^{31}P/^{1}H$ heteronuclear COSY). It is important to point out that the sequential resonance assignment methods via 2D NOESY and COSY generally require knowing the structure in advance (i.e. assuming a B-DNA double helix geometry). However, since we can unambiguously make some of the ^{1}H signal identifications by the $^{31}P/^{1}H$ heteronuclear COSY experiment, without recourse to any assumed initial geometry (10), we can check our assignments made by the H-1 sequential 2D NMR methodology. This is particularly important if the double helix possesses unusual geometry.

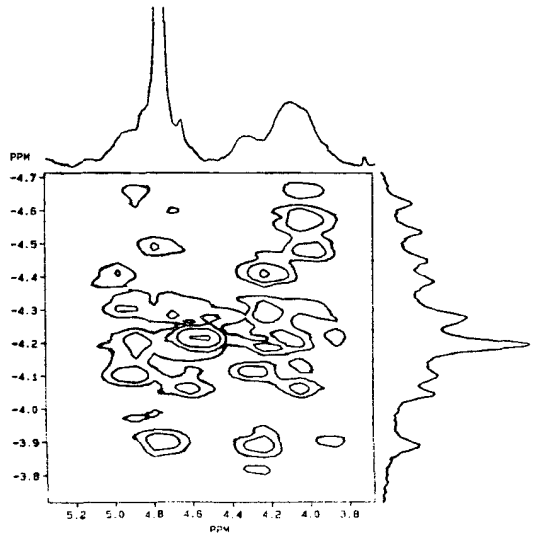

Figure 9. Two-dimensional ^{3i}P-^{1}H COLOC NMR spectrum of duplex 14-mer at 200 MHz (^{1}H). The COLOC (29) heteronuclear correlated NMR spectrum provides better sensitivity in spin systems with small coupling constants than the conventional 2D heteronuclear correlated (HETCOR) NMR spectrum (10, 20).

CONSTRAINED MOLECULAR MECHANICS CALCULATIONS OF DUPLEX GEOMETRIES

The relative intensities of the two-dimensional NOESY cross peaks, in the absence of spin diffusion and significant internal local motion, can provide information on the interatomic distances in macromolecules (30). Using the molecular mechanics energy minimization program AMBER (31), an idealized Arnott B-DNA geometry was constructed for duplex 4. Distances were derived from the relative intensities of the cross-peaks of the 2D NOESY spectrum of 14-mer 4. Starting from the idealized model-built duplex

structure, we used the molecular mechanics energy minimization routine of AMBER (31) to minimize the energy of the 14-mer with (Figure 10B) and without (Figure 10A) 54 NOESY-distance constaints. A simple harmonic potential error function was used for the distance constraints, although a flat well or skewed harmonic function likely better reflects the intrinsic accuracy of these NOESY distance constraints (32). As noted in Figure 10, while some differences are observed between the constrained and unconstrained minimized duplexes (particularly at the ends of the duplex where fraying of the strands is possible), the main features of the B-DNA duplex are retained in either calculation. This is not surprising since the energy minimization method often traps structures in local energy minima (32). It is now apparent that constrained molecular dynamics calculations may circumvent this problem (32). However, it is now quite feasible to use 2D NMR in conjunction with energy minimization/dynamics calculations to determine the three dimensional structure of oligonucleotides in solution.

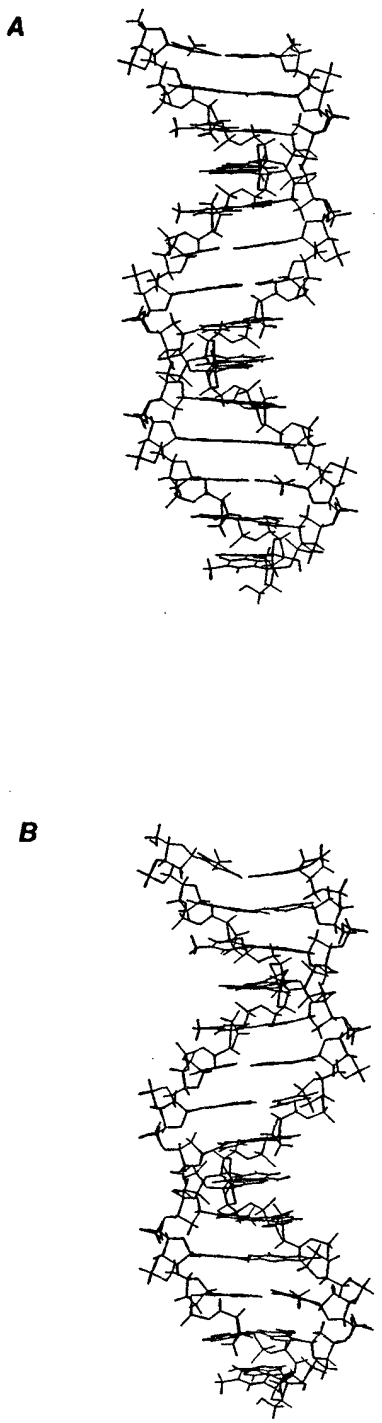

Figure 10. (A) Molecular mechanics energy minimized structure of B-DNA model built oligonucleotide 14-mer 4 using the AMBER program. (B) NOESY-distance constrained.

ACKNOWLEDGMENTS

Supported by the National Institutes of Health (GM36281). Support of the Purdue Biochemical NMR facility by NIH (RR01077) is acknowledged.

REFERENCES

1. Kearns, D.R., **Crit. Rev. Biochem. 15**, 237-290 (1984).
2. James, T.L., In "Phosphorus-31 NMR: Principles and Applications" (D. Gorenstein, ed.), Academic Press, Orlando, pp. 349-400 (1984).
3. Hare, D.R., Wemmer, D.E., Chou, S.H., Drobny, G., and Reid, B., **J. Mol. Biol. 171**, 319 (1983).
4. Feigon, J., Leupin, W., Denny, W.A., and Kearns, D.R., **Biochemistry 22**, 5930-5942, 5943-5951 (1983).
5. Frechet, D., Cheng, D.M., Kan, L.-

S., and Ts'o, P.O.P., **Biochemistry 22**, 5194-5200 (1983).
6. Pardi, A., Walker, R., Rapoport, H., Wider, G., and Wuthrich, K., **J. Am. Chem. Soc. 105**, 1652 (1983).
7. Broido, M.S., Zon, G., and James, T.L., **Biochem. Biophys. Res. Commun. 119**, 663-670 (1984).
8. Scheek, R.M., Boelens, R., Russo, N., Van Boom, J.H., and Kaptein, R., **Biochemistry 23**, 1371-1376 (1984).
9. Hilbers, C.W., Haasnoot, C.A.G., de Bruin, S.H., Joordens, J.J.M., van der Marel, G.A., and van Boom, J.H., **Biochimie 67**, 685-695 (1985).
10. J.M. Fu, S. Schroeder, C. Jones, D.G. Gorenstein, submitted.
11. Kumar, A., Wagner, G., Ernst, R.R., and Wuthrich, K., **J. Am. Chem. Soc. 103**, 3654-3658 (1979).
12. Havel, T.F., Kuntz, I.D., and Crippen, G.M., **Bull. Math. Biol. 45**, 665-720 (1983).
13. Gorenstein, D.G., In "Jerusalem Symposium, NMR in Molecular Biology" (B. Pullman, ed.), pp. 1-15, D. Reidel (1978).
14. Gorenstein, D.G., **Ann. Rev. Biophys. Bioeng. 10**, 355 (1981).
15. Gorenstein, D.G., **Prog. in NMR Spectrosc. 16**, 1-98 (1983).
16. Gorenstein, D.G., Editor, "^{31}P NMR: Principles and Applications", Academic Press, New York (1984).
17. Gorenstein, D.G., Kar, D., and Momii, R.K., **Biochem. Biophys. Res. Commun. 73**, 105 (1976); Gorenstein, D.G., Kar, D., Luxon, B.A., and Momii, R.K., **J. Am. Chem. Soc. 98**, 1668 (1976); Gorenstein, D.G., Findlay, J.B., Momii, R.K., Luxon, B.A., and Kar, D., **Biochemistry 15**, 3796 (1976).
18. Gorenstein, D.G., Goldfield, E.M., Chen, R., Kovar, K., and Luxon, B.A., **Biochemistry 20**, 2141 (1981).
19. Gorenstein, D.G., Luxon, B.A., Goldfield, E., and Vegeis, D., **Biochemistry 21**, 580 (1982); Gorenstein, D.G., Luxon, B.A., Goldfield, E.M., and Vegeais, D., **Biochemistry 21**, 580 (1982).
20 a) Shah, D.O., Lai, K., and Gorenstein, D.G., **J. Am. Chem. Soc. 106**, 4302 (1984). b) Gorenstein, D.G., Lai, K., and Shah, D.O., **Biochemistry 23**, 6717 (1984).
21. Petersheim, M., Mehdi, S., and Gerlt, J.A., **J. Am. Chem. Soc. 106**, 439 (1984).
22. J. Ott, and F. Eckstein, **Biochemistry, 24**, (1985) 253; J. Ott and F. Eckstein, **Nucl. Acids Res., 13** (1985) 6317-6330.
23. Stec, W.J., Zon, G., Egan, W., and Stec, B., **J. Am. Chem. Soc. 106**, 6077 (1985).
24. Patel, D.J., Pardi, A., and Itakura, K., **Science 216**, 581 (1982).
25. B.A. Connolly, B.V.L. Potter, F. Eckstein, A. Pingoud, and L. Grotjahn, **Biochem., 23** (1984) 3443.
26. M. Miyasaki, Ph.D. thesis, U. of Illinois at Chicago, 1986.
27. Calladine, C.R., **J. Mol. Biol. 161**, 343-352 (1982).
28. Dickerson, R.E., **J. Mol. Biol. 166**, 419-441 (1983).
29. Kessler, H., Griesinger, C., Zarbock, J. and Loosli, H.R., **J. Magn. Reson. 57**, 331-336 (1984).
30. Clore, G.M. and Groninborn, A.M., "Biomolecular Stereodynamics IV, Proceedings of the Fourth Conversation in the Discipline Biomolecular Stereodynamics," pp. 139-155, Adenine Press, NY (1986).
31. Weiner, S.J., Kollman, P.A., Case, D.A., Singh, U.C., Ghio, C., Alagona, G., Profeta, Jr., S., and Weiner, P., **J. Am. Chem. Soc. 106**, 765 (1984).
32. Nilsson, L., Clore, G.M., Gronenborn, A.M., Brunger, A.T., and Karplus, M.**J. Mol. Biol. 188**, 455 (1986); Kaptein, R., Zuiderweg, E.R.P., Scheek, R.M., Boelens, R., van Gunsteren, W.F.**J. Mol. Biol. 182**, 179.